CHAPTER 5: DISCUSSIONS

In Chapter 2, the experimental setup was discussed. In Chapter 3, a mathematical model for calculation of flow forming forces was presented. In the last chapter, the results of all the experimental trials and the tests have been presented. The present chapter presents the discussion of the results that have been reported in chapter 4.

5.1 Experimental Forces and validation of mathematical model

The in –situ measurement of flow forming forces in each case of Al6101 T6, Al2014 and Al7075 showed that the all the component of forces increases with increasing the percentage thickness reduction. This can be explained on the basis that as percentage thickness reduction increases, more material would undergo deformation per unit time. Thus higher power would be required to deform the material. The higher the power, higher will be force required. Hence, percentage thickness reduction is one of the most important factor affecting the flow forming forces.

Another important factor that affects the force is the thickness of the preform. Under the similar condition of mandrel speed, feed rate, and percentage thickness reduction, the preform having higher thickness would present a higher volume of material going under deformation per unit time as compared to preform having lower thickness.

Flow forming forces were found to increase with an increase in mandrel speed and feed rate. This can be explained on the basis that on increasing mandrel speed, the centrifugal force would be expected to increase. Due to the tapered section (attack angle section), a component of the force acts in the axial and radial direction, resulting in an increase in the axial and radial component of the force.

Further, increasing mandrel rpm would increase in axial feed [(mandrel rpm X feed rate (mm/ rev)]. As a result, there will be the development of a built-up edge before the roller. The development of built-up edge also increases the interaction between the material and roller and therefore, the forces were found to increase.

The mathematical model presented in chapter 3 has been validated with the experimental results in chapter 3. The mathematical model has been developed based on the upper bound method. The model assumes a linear variation between r and z was able to satisfy the conditions of kinematically admissible velocity fields and eased the mathematical calculations. The mathematical model involves two process efficiency terms η_a and η_r. The values of these terms can be obtained from some experimental trial runs. One limitation of the proposed mathematical model is that the end expression of the model does not take into account the effect of mandrel rpm and roller feed rate which got cancelled due to the nature of assumptions. The experimental results have shown that the above factor – mandrel rpm and the feed rate affects the flow forming forces. However, the effect of the above factors on flow forming forces has been reported to be smaller than the effect of thickness reduction.

The validity of the model was done by calculating the average values of the efficiency terms from the different experimental runs. The investigation results presented in the Table 3.1 to table 3.4 shows that the variation in the values of η_a and η_r is small in each aluminium alloys under consideration. However, the value of η_a and η_r was found to be different for each alloy. The close variation in values of η_a and η_r for different trial runs for an aluminium alloy shows the validity of the model.

The comparison of experimental force and forces predicted by the model for the Al6101 T6 samples has been presented Table 3.2. The value of the factors η_a and η_r have

been calculated based on results of Table 3.1. The result of comparison showed that the difference in predicted force and the experimental force was maximum 8.62 % in estimating the axial force and in case of radial force, the error was maximum 7.24 % under the present investigation. In both the cases, the predicted force was found to be lesser than the experimental force. The predicted model thus can be applied to the multipass flow forming of Al6101 T6 with acceptable accuracy within 10 % range.

The comparison of experimental force and forces predicted by the model for the Al7075 heat treated samples has been presented in Table 3.3. The value of the factors η_a and η_r have been calculated based on results of Table 3.2. The result of comparison showed that the difference in predicted force and the experimental force was maximum 9.08 % in estimating the axial force and in case of radial force, the error was maximum 10.5 % under the present investigation. In both the cases, the predicted force was found to be higher than the experimental force. The above errors were found to be in the first pass of the multipass 7F04 sample. The error was found to be decreased in the successive passes. The probable reason of overestimation could be the higher tensile strength of the final flow formed sample that was taken for estimation of force. The tensile strength of specimen of intermediate pass would be expected to be lower than the tensile strength of the final flow formed sample. Another reason can be the values of η_a and η_r which was the chosen as the average values of the range tabulated in Table 3.2. The values of Table 3.3 also shows that the difference between the experimental force and the predicted force decreases for the successive passes. In second and third passes, the experimental force was found to be slightly higher than the predicted force. This may be due to the increased tensile strength of the flow formed product after the first pass that has resulted in decreasing the difference that was observed in the first pass. The complex nature of the process and inability of the proposed model to account the effect of mandrel rpm and feed rate would have resulted in

experimental force being higher than the predicted force. The results of the mathematical model and the experimental results when compared shows a variation within 10% which is acceptable considering the absence of any standard data in the open-access till date.

The comparison of experimental force and forces predicted by the model for the Al2014 heat treated samples has been presented in Table 3.5. The value of the factors η_a and η_r have been calculated based on results of Table 3.5. The values of η_a and η_r found in case of Al2014 heat treated samples was found to be different than that obtained in the Al7075 heat-treated sample and Al6101 T6. This may be due to the different feed rate and mandrel rpm that was used in the investigation of Al2014 samples. However, the variation in η_a and η_r values in the different trials is found to be in close range of $\pm$ 0.05 from their mean value. This validates the model prediction.

The mathematical model thus predicts forces with an error of 10% in the present investigation. The errors can be minimized by optimizing the values of the two process efficiency terms η_a and η_r. The values of these terms has been obtained from the experimental trial runs. The values were found to be different for different alloys as the values takes into account the errors that have been induced due to the change in tensile strength values, the change in mandrel rpm and the feed rate.

The values of η_a and η_r can be optimized to give better result by increasing the number of trial runs. In the present investigation, the number of trials was limited to around 5 trials.

The values of η_a for Al6101 T6 have been found to be less. Similar results were also reported by several other researchers [56][66] for Al6XXX series. The value of process efficiency factor η_r are found to be close to 1 in case of flow flowing of Al6101 samples. This validates the assumption that circumferential force was much less significant in flow forming of axisymmetric work pieces.

The present mathematical model have been applied for three aluminium alloys used. The model can be used for other aluminium alloys and other metal alloys. In all case, the present model can be used as a reference to predict a flow forming force at the start of the trial. It has been proposed that to present model can be more efficient if initial trials are done on standard specimen with definite process plan. The process parameters such as mandrel rpm, and feed rate, should be decided by the user and should not be changed for the process for the entire lot of preform. The errors in the predicted force and experimental force first dew trials are noted. Then, the using computational technique, the error values in η_a and η_r can be converged to optimized value so that error becomes minimum. Then using the optimized values of η_a and η_r, the flow forming forces of another 5-10 samples are compared. Finally, when the values of η_a and η_r becomes consistent, these can be applied for all the lot available.

5.2 X- ray diffraction results

X- ray diffraction analysis was done for the various heat treatable aluminum alloy (7xxx, 6xxx and 2xxx series) specimen. Analysis of peak depicts the presence of α-Al solid solution phases (PDF#85-1327) along with GP Zone ($MgZn_2$)(PDF#65-3578), η' and η (PDF# 77-1177), $CuAl_2$ intermetallic compounds (PDF#89-1980) in the 7075-T6 heat treated aluminum alloy. Intensity of the transition precipitates (GP-Zones, η' and η) reduces while giving 20% and 40% deformation to the as received 7075-T6 aluminum alloy. The average crystallite size (D) and lattice microstrain (ε) values dislocation density has been given in the Table 5.1. The transition precipitates in the 2xxx and 6xxx series aluminum alloys are Al_2Cu and Mg_2Si.

The values of lattice microstrain and dislocation densities were found to increase in flow forming process, as compared to undeformed samples. This is an expected result as flow

forming is a cold forming process and an intrinsic feature of cold deformation in formation of dislocations which increases the dislocation density. Also, as the movement of dislocations are obstructed, lattice microstrain is expected to be higher. The cold deformation also decreases the grain size of the crystal. Hence, the crystallite size in flow formed product was found to decrease as compared to undeformed samples. This is evident from Table 5.1.

Table 5.1: Lattice microstrain, crystallite size, and dislocation density of the various heat treatable aluminum alloys

Serial No	**Specimens**	**Crystallite size(Å)**	**Lattice microstrain(%)**	**Dislocation density(x10^{17}/m^2)**
01	7075- undeformed	14.5	12.2	29.3
02	7075-20% Def	8.02	14.01	55.15
03	7075-66.67% Def (7F04)	7.64	20.0	71
04	2014 Deformed	6.50	15.38	73
05	2014 As recived	11.7	12.71	37
06	6101 As received	9.62	13.27	46
07	6101 Deformed	5.11	18.60	102.38

5.3 EBSD Analysis

EBSD analysis was done on 10 samples. The inverse pole figure, grain size distribution and the misorientation angle data for each sample has been reported in chapter 5. The data, presented in chapter 5, clearly suggested the change in crystal orientation during the flow forming process. The proportion of grains oriented along <101> direction was found to

increase. This is because the alloys taken under consideration are FCC and <101> represents slip direction of the FCC crystals. The grain size distribution data reaffirms that that grain refinement takes place during flow forming process.

Misorientation data showed number fraction of low angle grain boundary increases when the samples were flow formed. With high proportion of low angle grain boundaries, higher proportion of fine grains, the movement of dislocations are greatly hindered. As a result the physical properties such as hardness, tensile strength are expected to increase while ductility and percentage elongation decreases.

5.4 Microhardness test analysis:

Hardness variation in Al6101, Al7075 and Al2014 samples are shown in Figure 4.45 and Figure 4.51 respectively. The results shows that the Vickers microhardness of the flow formed product and the undeformed preforms which was due to fine grain size. This was also expected as hardness increases as tensile strength increases [94], [95]. The result showed that the Vickers microhardness of the flow formed product was higher than the undeformed sample.

In as received T6 condition, the average hardness of the sample was around 130 HV while in average grain size in the as received preform was 46.2μm. Due to high hardness, the roller was found to slip during the floe forming process leading to failure without much elongation. Measurement of residual stress showed that in 2014 T6 samples were found to be 109.8 MPa. Presence of tensile residual stress means that the hardness value without residual stress be more as tensile residual stress generally hardness while compressive residual stress would increase the hardness value [95]–[98][99]. The residual stress in preform was found to be 9MPa. This suggests that the annealing was not complete and samples required more annealing time. The hardness of the annealed samples were around

42 HV. However, in hardness value increases from 42 HV in annealed samples to 87.41 HV in 2014-5

5.5 Defects in Flow forming

Common defects that have been reported in chapter 4 were diametral growth, roller marks, wrinkling, crack formation, and ovality. The diametral growth was found to be the most common defect that was present in most of the samples under consideration.

5.5.1 Diametral growth

The diametral growth was found to increase as the residual stress increased. Flaring of ends and diametral growth in 7F01 and 7F02 samples showed that as the infeed was increased, the forces were increased. No appreciable elongation was observed but the diameter of the samples was increasing resulting in the formation of a gap between the mandrel and the inner portion of the workpiece. This concludes that higher forces induce higher diametral growth.

5.5.2 Chip formation

Chip formation (Figure 4.37) was found during the initial experimentation. This can be due to either material inhomogeneity or due to skidding or ploughing interaction between the roller and the workpiece. In the present investigation, same material is used for all investigation. Hence, material inhomogeneity does not account for the chip formation. In our investigation, it was found that the under loading condition, lateral movement of roller was taking place due to which the free rotation movement of roller was hindered. This was found to create a ploughing interaction in the surface of the roller which resulted in chip formation. The defect was found to be corrected once thrust bearing was placed.

5.5.3 Distortion of the tube

Distortion of the tube has been found in some product. This may be due to buckling of mandrel under radial load or due to poor support at tailstock end. In our investigation it has been found that the end of mandrel held in chuck of head stock has been strongly held but the other end of mandrel supported at tailstock end, was deflecting under radial load due to improper support.

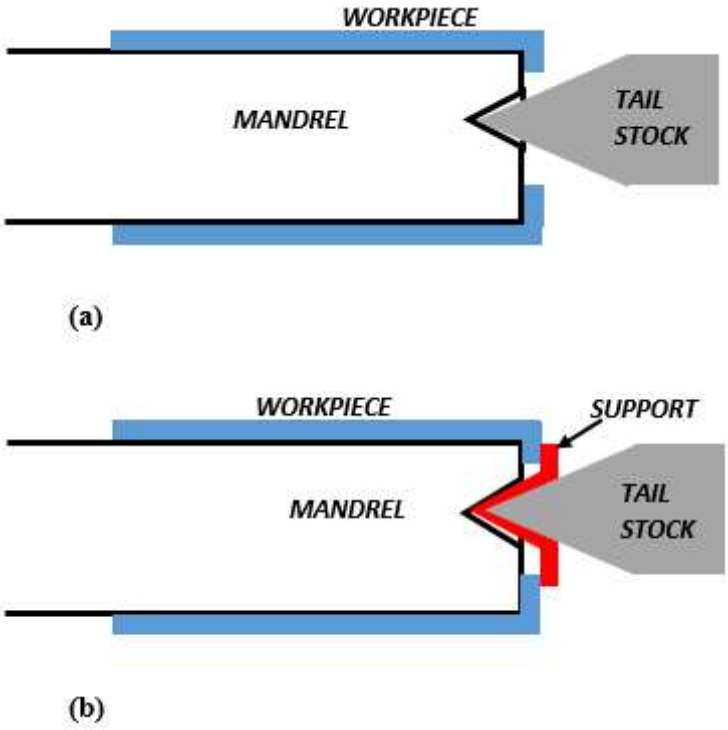

Figure 5.1: Mandrel Support at tail support (a) initial design (b) modified design by introducing a support

The problem was accounted to the small contact region between the tail stock and the centre punch in the mandrel. The problem was corrected by introducing a support as shown in Figure 5.1 (b). The support was found to increase the surface area of contact leading to

better resistance to the radial load. The support also reduced wear and tear of the mandrel's centre hole.

5.6 SEM Fractography of tensile specimen and cracked specimen

SEM fractography was done on 5 failed specimens and 8 tensile specimens that failed during tensile testing. The fractograph of failed specimen showed in general, dimple formation except in Al2014 specimen, which showed different morphology. This shows that the failure mode was brittle in nature. In most of the failed specimen, presence of secondary phase particles are seen. These particles movement results in void formation. When more than on void coalesce, this may lead to crack formation. In fractograph of 7F03 (Figure 4.42) some weld like morphologies are seen. This may be due to localised melting of material under high roller load and high localised heating due to friction. However, the temperature of this zone was not detected by infrared thermometer.

In the fractographs of failed tensile specimen, the presence of dimples were most common morphologies in all, showing the ductile mode of fracture. However, the morphologies of dimple was different. In general, a large, deep dimple represents higher ductility and higher formability whereas a small shallow dimples represents lower ductility of the material and hence lower formability. Flow formed material undergo cold deformation resulting in fine grain structures and thus are expected to have high low ductility. Therefore, the fractograph of flow formed material would be expected to show shallow or small dimples as compared to the preform material which is not flow formed. Presence of crack in some samples can be either due to secondary particle segregation which results in void and ultimately crack formation or it can be due to inhomogeneous deformation.[100].

CHAPTER 6: CONCLUSIONS AND FUTURE SCOPE OF WORK

This chapter summarizes important conclusions and comprises suggestions for future research.

6.1 Summary

This investigation takes the challenge to develop a setup for flow forming operation by modifying an old lathe machine with minimum expense. This investigation tries to bring out all aspects of developing an in-house facility for flow forming operation. The investigation tells about the design and fabrication of roller assembly, mandrel and preform. Though the investigation was done on soft alloys, the methodology can be easily employed to hard to deform alloys. A robust lathe machine can be used to perform flow forming operations on harder substances. One very important aspect of this investigation is that it brings out the various defects that can normally arise during the flow forming process and proposes their root causes and probable solution. The results of this investigation are expected to be very useful for any small scale industry that wants to start a flow forming operation on a small scale.

6.2. Summary of Investigation of Flow forming

The present investigation had utilized the developed in-house facility to perform the experimental study on different alloys of aluminium viz. Al6101 T6, Al7075 and Al2014. This study is important as very little researches are available in the literature on these alloys.

The present investigation brought about the challenges in flow forming of different aluminium alloys. The important conclusions are presented below

- The present investigation was able to develop the setup and perform flow forming operation in an existing fabrication setup by utilizing an old lathe machine.
- The investigation discusses the challenges in setup development and proposes solutions to overcome the challenges. The investigation has provided information about the part drawings used in developing the setup. The investigation also tried to bring about the various defects related to the setup, such as bending of job and slipping of roller over the preform, and proposed ways to minimize the error.
- The investigation has tried about the various defects such as diametral growth, chip formations, crack formation, etc., that are related to process parameters and the material of preform and tried to propose probable root cause.
- In the investigation, flow forming operation was done on three different aluminium alloys – Al6101, Al2014, and Al7075. The investigation showed that flow forming operation in the T6 temper condition of Al6101 was possible in the present setup. However, under similar conditions, flow forming of Al2014 and Al7075 in T6 temper condition was difficult and caused problems such as bending of the mandrel, rotation of tool post etc. Hence, the flow formability of Al6101 T6 preform was found to be better than Al2014 T6 and Al7075 T6 preforms. Further, the investigation also showed that the rigidity of the machine would also be a deciding factor in deciding the infeed (thickness reduction per pass).
- In the present investigation, flow forming of preforms of Al7075 T6 and Al 2014 T6 samples showed poor formability. Almost all the samples failed within 20% elongation. So, heat treatment of Al7075 T6 and Al2014 T6 samples before

deformation is recommended. In the present investigation, heating Al7075 T6 perform at 470 ºC for 3 hours and heating Al2014 T6 at 413ºC for 2 hours has been found to increase the flow formability of the respective materials. After the flow-forming operation, the heat-treated preforms showed more than 100% elongation.

- The investigation also showed that multipass flow forming is a better alternative than single-pass flow forming for higher overall thickness reduction. However, the time of production would be higher for multipass flow forming. The thickness was reduced from 2 mm to 0.4mm in the present investigation. The results for each alloy- Al6101, Al7075 and Al2014 under investigation showed an overall higher thickness reduction greater than 60%, which was impossible in a single pass due to high flow forming forces and resulting torque distorted the mandrel. The result of the investigation for each alloy under study showed that multipass flow forming with decreasing infeed in successive passes would result in an overall larger thickness reduction without failure.
- Flow formed product characteristics showed a decrease in crystallite size, increased dislocation density, and more low angle grain boundaries fractions than the preform. The increase in dislocation density was more for higher thickness reduction.
- The mathematical model proposed in the present investigation provides the basis to start the flow forming process planning. The values obtained from the model can be used as a reference for designing of parts. The efficiency terms used in the model have to be optimized to minimize errors in the prediction. The values for these depend on the preform mechanical and metallurgical properties and the process parameters such as mandrel rpm and feed rate that has not been figured out in the proposed model.

- The proposed model is adaptive because it can be used for the different alloys by using the optimized values of η_a and η_r for that particular material following the process proposed in section 5.1

6.3 Suggestions for future work:

Flow forming is a very important process, but this process is not achieved much acceptance, mainly due to a lack of knowledge about the process. The following suggestions for future investigation are made based on the present investigation.

(a) Detailed study of creep and fatigue behaviour of flow formed product

(b) Corrosion behaviour of the flow formed product.

(c) Develop an expert system for different materials such as alloys, cladded, and reinforced materials.